Neurobiology of Sleep and Circadian Rhythms 5 (2018) 37–51

Contents lists available at ScienceDirect

Neurobiology of Sleep and Circadian Rhythms

journal homepage: www.elsevier.com/locate/nbscr

Research paper

Mathematical modeling of sleep state dynamics in a rodent model of shift work

Michael J. Rempe[a,b,*,1], Janne Grønli[a,c], Torhild Thue Pedersen[c], Jelena Mrdalj[c], Andrea Marti[c], Peter Meerlo[d], Jonathan P. Wisor[a,e]

[a] Sleep and Performance Research Center, Washington State University, Spokane, WA, USA
[b] Dept. of Mathematics and Computer Science, Whitworth University, Spokane, WA, USA
[c] Department of Biological and Medical Psychology, University of Bergen, Bergen, Norway
[d] Groningen Institute for Evolutionary Life Sciences, University of Groningen, Groningen, The Netherlands
[e] Elson S. Floyd College of Medicine, Washington State University, Spokane, WA, USA

ABSTRACT

Millions of people worldwide are required to work when their physiology is tuned for sleep. By forcing wakefulness out of the body's normal schedule, shift workers face numerous adverse health consequences, including gastrointestinal problems, sleep problems, and higher rates of some diseases, including cancers. Recent studies have developed protocols to simulate shift work in rodents with the intention of assessing the effects of night-shift work on subsequent sleep (Grønli et al., 2017). These studies have already provided important contributions to the understanding of the metabolic consequences of shift work (Arble et al., 2015; Marti et al., 2016; Opperhuizen et al., 2015) and sleep-wake-specific impacts of night-shift work (Grønli et al., 2017). However, our understanding of the causal mechanisms underlying night-shift-related sleep disturbances is limited. In order to advance toward a mechanistic understanding of sleep disruption in shift work, we model these data with two different approaches. First we apply a simple homeostatic model to quantify differences in the rates at which sleep need, as measured by slow wave activity during slow wave sleep (SWS) rises and falls. Second, we develop a simple and novel mathematical model of rodent sleep and use it to investigate the timing of sleep in a simulated shift work protocol (Grønli et al., 2017). This mathematical framework includes the circadian and homeostatic processes of the two-process model, but additionally incorporates a stochastic process to model the polyphasic nature of rodent sleep. By changing only the time at which the rodents are forced to be awake, the model reproduces some key experimental results from the previous study, including correct proportions of time spent in each stage of sleep as a function of circadian time and the differences in total wake time and SWS bout durations in the rodents representing night-shift workers and those representing day-shift workers. Importantly, the model allows for deeper insight into circadian and homeostatic influences on sleep timing, as it demonstrates that the differences in SWS bout duration between rodents in the two shifts is largely a circadian effect. Our study shows the importance of mathematical modeling in uncovering mechanisms behind shift work sleep disturbances and it begins to lay a foundation for future mathematical modeling of sleep in rodents.

1. Introduction

Night-shift workers are awake at times when their sleep propensity is high and are required to sleep when sleep propensity is low. As a whole, this work population reports more sleep difficulty than the general public (Ursin et al., 2009), and night-shift workers report more insomnia than day- or evening-shift workers (Pilcher et al., 2000; Torsvall et al., 1989). Recent studies have shown that night-shift workers show a higher propensity for occupational errors and accidents (Ursin et al., 2009; Van Dongen et al., 2017), and in the long run, night-shift workers also have increased risk of developing a wide range of adverse health outcomes, such as cancer, cardiovascular disease, diabetes and gastrointestinal disorders (Kecklund and Axelsson, 2016; Knutsson, 2003). In many cases, the relationship between shift work and health issues may be mediated by shift work-related sleep problems (Knutsson, 2003).

Sleep is a state characterized by well-defined changes in brain activity as seen in the electroencephalogram (EEG). Optimal sleep quality

* Corresponding author at: Sleep and Performance Research Center, Washington State University, Spokane, WA, USA.
E-mail address: m.rempe@wsu.edu (M.J. Rempe).
[1] MJR supported by a Whitworth University STEM fellowship.

https://doi.org/10.1016/j.nbscr.2018.04.002
Received 30 June 2017; Received in revised form 19 April 2018; Accepted 20 April 2018
Available online 28 April 2018

is regulated by a sleep homeostatic process (process S) and the endogenous circadian clock (Process C) (Daan et al., 1984). Process S is a mathematical representation of sleep pressure that builds up during wakefulness and dissipates with time in sleep. The amount of slow waves in the EEG of slow wave sleep (SWS) is considered a good indicator of sleep homeostasis (Dijk et al., 1987; Franken et al., 1991; Huber et al., 2000). The second component, the oscillatory Process C, also plays a role in the timing of sleep and wakefulness, and is controlled and coordinated by the circadian pacemaker located in the suprachiasmatic nuclei (SCN) of the brain. The SCN synchronize daily rhythms in numerous physiological functions, including core body temperature. Process C also modulates alertness and cognitive performance, even as sleep need builds. Although Process S and Process C are not specific measurable quantities, homeostatic aspects of sleep as well as circadian aspects of sleep can be altered experimentally. Process S can be altered by enforcing sleep restriction, for instance, and Process C can be altered by changing the light/dark cycle or by lesioning the SCN. Alterations in either or both of these two processes results in changes in subsequent sleep structure (A. Borbély et al., 2016; Edgar et al., 1993).

Night-shift work induces a mismatch between work demands and the homeostatic and circadian factors that promote sleep drive. The immediate effects of night-shift work are often manifested as decrements in alertness and cognitive performance on duty, and insufficient sleep after work (Folkard and Tucker, 2003; Gumenyuk et al., 2014; Kazemi et al., 2016). One explanation is a temporal mismatch between sleep opportunities and circadian rhythmicity. Working during the circadian alertness nadir causes state instability, resulting in lapses, slowing of cognitive processes, microsleeps or sleep attacks measured by EEG activity (Doran et al., 2001). Although high homeostatic sleep pressure makes it relatively easy to fall asleep after night-shift work, the circadian system at this time facilitates wakefulness. As a result, the daytime sleep is usually shortened even in the face of remaining homeostatic sleep drive. The dissipation of homeostatic sleep drive after night-shift work is thus incomplete compared to sleep following day-shift work (Torbjörn Akerstedt and Wright, 2009). Understanding this phenomenon is increasingly important as sleep problems related to the work schedule may underlie acute cognitive impairments or long-term health risks associated with shift work.

Recently, we established a rodent model of shift work by subjecting rats to enforced ambulation in slowly rotating wheels for 8 h per day, either at the time of day when the animal is primed for sleep, ("rest-work"; to simulate night-shift work) or at the circadian time when the animal is physiologically primed for wakefulness ("active-work"; to simulate day-shift work). Rest-work, in contrast to active-work, forces subjects to recover sleep during the endogenous active phase. Based on this model, we have observed a progressive intrusion of spontaneous cortical slow waves and microsleeps during rest-work across four consecutive days, which was not observed during active-work (Grønli et al., 2017). Similar findings have been observed in human studies, and likely contribute to decreased alertness during the night shift (T. Akerstedt et al., 1987; Torsvall and Akerstedt, 1987; Torsvall et al., 1989). We also found that rest-work does not constitute a simple sleep deprivation, but instead causes a redistribution of sleep. The sleep lost during work in the resting phase is largely compensated by more sleep in the normal circadian activity phase. Importantly, the distribution of sleep is not only affected by working in the resting phase but also by working in the active phase (since subjects working during the active phase do get some sleep during the work period). Overall, this rodent model of shift work increased the daily time awake and decreased the daily time in sleep in both active-workers and rest-workers as compared with the undisturbed baseline condition. The total Slow Wave Energy in non-Rapid Eye Movement (NREM) sleep during the 4-day work schedule was not different in rest-workers from that of active-workers (Grønli et al., 2017). Therefore it does not appear that the sleep deprivation induced to the rest-workers by initiating their work at zeitgeber time 2 (ZT2) had a significant effect as compared to the active-workers.

While previous research clearly demonstrates that night-shift work has a major impact on sleep architecture, the exact mechanisms underlying these changes are not yet fully understood. Important questions remain, particularly: 1) Does the simulated work shift induce changes in Process S as compared to baseline? 2) What are the mechanisms underlying differences in sleep architecture between active-workers and rest-workers during the workweek? Our aim in the current study is to answer these questions through the development and analysis of mathematical models. We use two different mathematical models to quantify differences between simulated night- and day-shift work and to investigate putative mechanisms responsible for the changes in sleep architecture. For the first research question, we apply a recently developed simple homeostatic model of sleep (Process S) (Rempe and Wisor, 2014). We apply this model to determine if slow wave activity (SWA) time dynamics change between rest-workers and active-workers during work days, as compared to baseline. To address the second question, we develop a hybrid model that makes use of a stochastic process to determine sleep state and bout duration at any given time in polyphasic rodents. The sleep state is determined probabilistically within constraints set by the homeostat and a circadian rhythm. The standard two-process (Processes S and C) model is effective at tracking trends in SWA on the time scale of hours to days. This more advanced mathematical framework presented in this paper predicts the shorter-term dynamics of sleep and wakefulness and allows us to make predictions about the mechanisms underlying those dynamics.

2. Materials and methods

2.1. Ethical approval

This study was carried out in accordance with Norwegian laws and regulations, and The European Convention for the Protection of Vertebrate Animals used for Experimental and Other Scientific Purposes. The protocol was approved by the Norwegian Animal Research Authority (permit number: 2012463).

2.2. Data collection

Male Wistar rats (nTach:WH, Taconic, Silkeborg, Denmark) were kept under 12:12 light-dark (LD) conditions with gradual transitions between the light and dark phases, from 0600 to 0700 for lights-on and from 1800 to 1900 for lights-off, respectively. Accordingly, 0600 was labelled as lights on (zeitgebertime, ZT0) and 1800 was labelled as lights off (ZT12). To simulate shift work in humans, rats were exposed to enforced ambulation for 8 h per day, centered either in the rats' normal active phase (active-workers "AW"; ZT14-22; n = 12) or in the rats' normal rest phase (rest-workers "RW"; ZT2-10, n = 15). The animals were placed in automatically rotating wheels (Rat Running Wheel, TSE running wheel system, Bad Homburg, Germany; 24 cm diameter; 3 rpm; a total of 1440 revolutions per session; yielding 1.086 km of linear distance) equipped with feeders to provide food and water ad libitum. In the 16 h intervals between enforced ambulation sessions, all animals remained undisturbed in their home cages. All wheels, feeders and water bottles were cleaned with a 5% ethanol solution after each workday. Work schedules were repeated for four days. See (Grønli et al., 2017) for more details.

Electroencephalogram (EEG) and electromyogram (EMG) were continuously monitored throughout a 24 h undisturbed baseline period, and through the 4-day work protocol (workdays W1 to W4). See Fig. 1 for an overview of the protocol.

For assessment of sleep-wake patterns, the animals underwent surgery for the implantation of transmitters to record EEG and EMG (4ET and F40-EET, Physiotel, Data Sciences International; St. Paul, MN). Telemetry signals were collected through receivers (RPC-2/RPC-3, Data Sciences International) placed directly beneath the animals' home cage

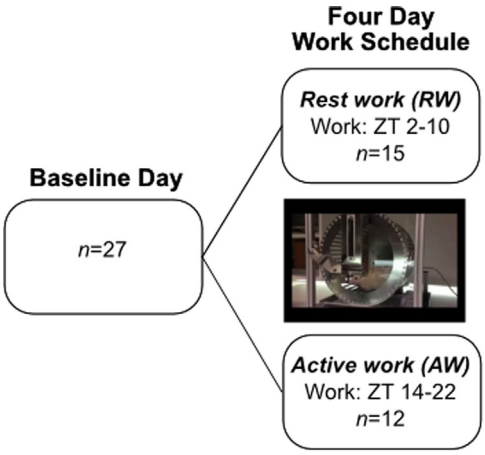

Fig. 1. Overview of the experimental design. All rats underwent a 24-h baseline recording in an 12/12 LD cycle. The animals were then split into two groups: Active-workers (AW) and Rest-workers (RW). Each animal underwent 8 h of forced ambulation on a motorized running wheel. ZT: Zeitgeber time.

or next to the rotating wheel during forced ambulation. The EEG and EMG signals were visually inspected and classified for sleep state using Neuroscore software (version 2.0.1, Data Sciences International). Wakefulness, SWS and Rapid Eye Movement sleep (REMS) were manually classified in 10-s epochs. For the purpose of manual scoring, based on criteria from Neckelmann and Ursin (Neckelmann and Ursin, 1993), the EEG signals were filtered with high-pass at 0.5 Hz and low-pass at 35 Hz. EMG signals were filtered with high-pass at 5 Hz. In addition to the time spent in sleep and wakefulness, the spectral characteristics of the EEG were analysed on unfiltered EEG signals by offline Fast Fourier Transform analysis, and artefacts were removed. EEG SWA was calculated for each epoch as the spectral power in the 1–4 Hz range. See (Grønli et al., 2017) for more details. Some of the experimental data presented in the current study (Fig. 5 panel A, Fig. 6 panels B and C) were published in (Grønli et al., 2017).

2.3. Simple homeostatic model

To quantify the dynamics of SWA during SWS we employed a previously published modeling framework (Rempe and Wisor, 2014). Following the approach of Franken (Franken et al., 2001), after finding all 5 min overlapping segments that consisted of at least 90% SWS, we computed and plotted the median power in the EEG signal in the 1–4 Hz range during these segments. To quantify the temporal dynamics of SWA during SWS, we fit these data points with a simple homeostatic model (Process S) that rises during epochs classified as wakefulness or REMS and declines during SWS.

The equations for Process S are the following:

$$S_{t+1} = UA - (UA - S_t)e^{\frac{-\Delta t}{T_i}} \text{ Wake or REMS}$$

$$S_{t+1} = LA + (S_t - LA)e^{\frac{-\Delta t}{T_d}} \text{ SWS}$$

The upper and lower asymptotes (UA, LA), were found (separately for each recording) in the same way as in a previous study (Franken et al., 2001): UA was chosen as the 99% level of the distribution of SWA during SWS. The lower asymptote, LA, was chosen as the intersection of the histogram curves of SWA during REMS and SWA during SWS. The only free parameters left in the model were the time constants: Ti and Td.

The rates at which S rises and declines (Ti and Td respectively) were optimized by minimizing the Root Mean Square Error between the model output and the data. Process S was fit to each individual recording, and time constant values were optimized for two different subsets of each recording: the baseline day and the workdays. The asymptotes that Process S approached were fixed constants, but differed between recordings. The average values of Ti and Td reported here are averages of the optimized values for each recording.

2.4. Markov chain model

We employ an adapted version of a Markov Chain model put forth by (Kemp and Kamphuisen, 1986). A Markov Chain uses random numbers (with constraints) to simulate transitions between sleep states as well as the amount of time spent in each state. When the model is in one state, two computations must be made: first, how long does the current episode last, and second, which state does it transition to next. The duration of episodes and the probability of transitioning to another state are functions of a homeostatic process and a circadian process (Process S and Process C, respectively), from the two-process model of sleep regulation (Achermann and Borbély, 1994; Borbély et al., 2016; Daan et al., 1984), but with different parameter values for the time constants for Process S. We model sleepiness as S-C and alertness as 1-(S-C) following other published work using the two-process model (Achermann and Borbély, 1994; Borbély and Achermann, 1992; Daan et al., 1984; Folkard and Akerstedt, 1989).

2.4.1. Modeling accurate episode durations

To model the time spent in a particular state, we first determined the probability distribution of episode durations using all the baseline experimental data (both AW and RW) and we used MATLAB's `distfit` tool to optimize the parameters of the distribution to fit the data. To generate random numbers from these probability distributions we used MATLAB's `makedist` function.

For REMS episodes during baseline we found that the probability distribution of their durations was best fit using a Burr Type II distribution (See Fig. 3**G**) which has the following probability density function:

$$y = \frac{\frac{kc}{a}\left(\frac{x}{a}\right)^{c-1}}{\left(1 + \left(\frac{x}{a}\right)^{c}\right)^{k+1}}$$

where the optimal parameters values were found to be a = 172.817, c = 2.629, k = 4.751. This probability was found using all of the REMS bouts during baseline and did not take into account time of day. We found (see Fig. 3**J**) that REMS episode durations during the baseline day are functions of sleepiness (Process S minus Process C). That is, when sleepiness rose throughout the day, REMS episodes tended to get longer. To account for this dependence on sleepiness, we modeled REMS episode durations as $y^*\alpha_R^*$sleepiness where α_R is a constant scaling factor whose value was optimized (see section "Optimizing parameter values").

For SWS episode durations during baseline we also found that the best type of probability distribution to fit the data was a Burr Type II distribution (Fig. 3**F**). In this case, the optimized parameter values are: a = 17.7113, c = 4.103,k = 1.483. Similar to REMS episodes, we found that during baseline SWS episode durations were not constant, but were longer when sleepiness was high (Fig. 3**I**). Therefore, we modeled SWS episode duration the same way as REMS duration: $y^*\alpha_S^*$sleepiness where α_S is a constant scaling factor whose value was optimized (see section "Optimizing parameters").

Consistent with previous studies (Lo et al., 2004), wake episodes in the baseline portion of the data were better fit with a power law distribution than an exponential distribution (Log likelihood value of -2137 vs -2159, Fig. 3**E**). Using MATLAB's `distfit` tool, the power law distribution is formulated as follows:

$$y = \left(\frac{1}{\sigma}\right)\left(1 + k\frac{(x-\theta)}{\sigma}\right)^{-1-\frac{1}{k}}$$

where the optimal parameter values were found to be: k = 0.231707, σ

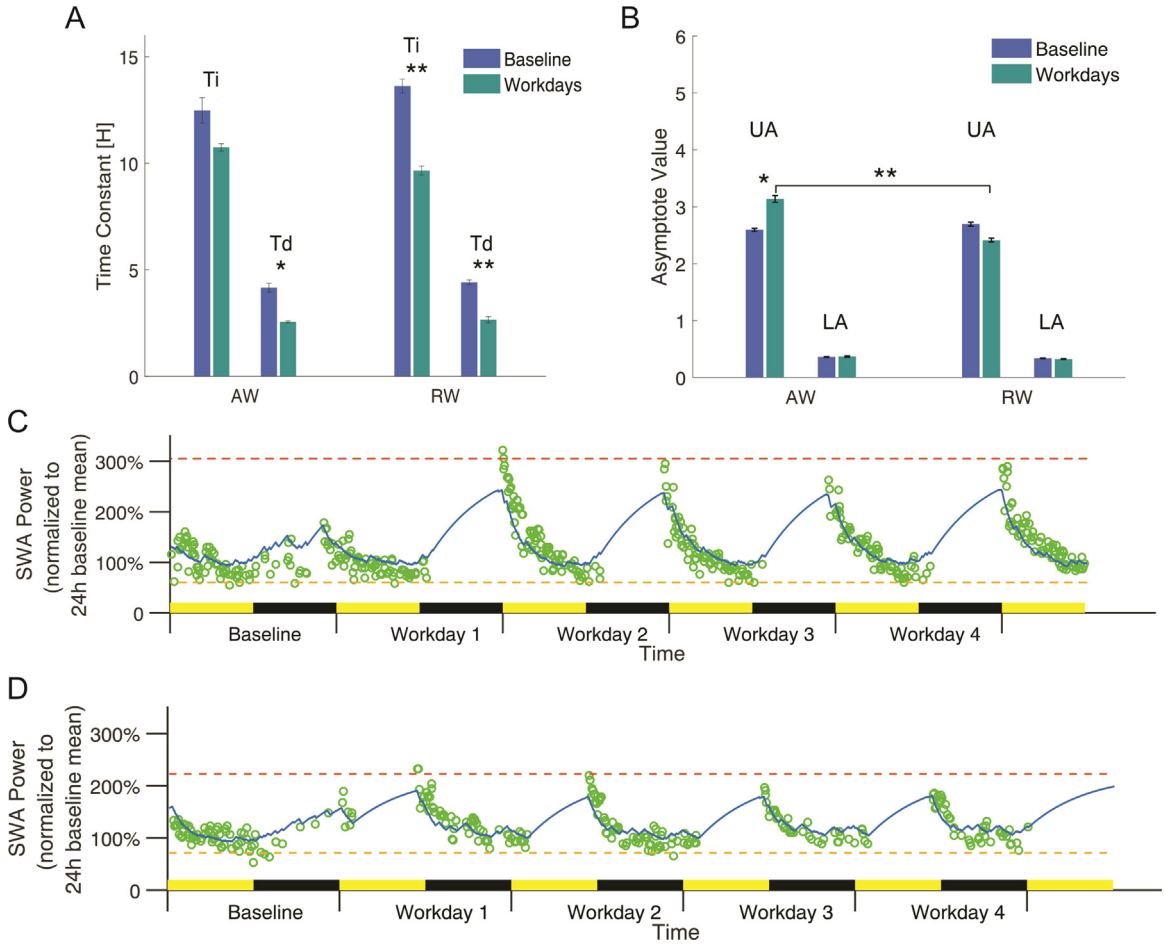

Fig. 2. A homeostatic model (Process S) quantifies differences in sleep slow wave dynamics between baseline days and work days. A When optimally fit to data points representing median delta power (1–4 Hz) during 5-minute episodes of slow wave sleep, both the rising time constant (Ti) and the decay time constant (Td) were significantly different between the baseline day and the workdays for the Rest-Workers (RW) group. Only Td was significantly different between baseline and work days for the Active-Workers (AW) group. **B** The lower asymptote values (LA) were the same for both AW and RW groups during baseline and during the workdays. The upper asymptote values (UA) was significantly larger during the work period for the AW group, but not the RW group. Also, UA was significantly larger during the work period for the AW group as compared to the RW group. Representative fits of the Process S model to data from one recording from the AW group (panel **C**) and one recording from the RW group (panel **D**). In the lower two panels data were normalized to the mean value during the 24 h baseline. Optimal values for Ti and Td were found using the Nelder-Mead method. Alternating yellow and black bands indicate the timing of light and dark intervals, respectively. *p < 0.05, **p < 0.01 unpaired t-test.

= 217.976, and θ = 1. The parameter θ sets the lower bound (in terms of epochs) for the wake distribution. In our experimental data we found that wake episode duration during baseline was a function of alertness (Fig. 3**H**). Consistent with how we modeled REMS durations and SWS durations, we modified this baseline distribution by multiplying it by the alertness measure (1-(S + C)) with a scaling factor. During work episodes, the model was forced to remain in the wake state regardless of the output of the Markov Chain model.

Interestingly, the same report of episode durations (Lo et al., 2004) showed a "hump-like tail" in the distribution of wake episode durations at large time scales. This means that especially long wake episodes are more likely than the power law would predict. In fact, their data show that long episodes, between about 5 min and 30 min are equally likely, although none of these long episodes are very common. This feature was thought to be caused by consolidated wakefulness due to physical activity. To incorporate this feature into the model, we assumed that long wake episodes were more likely when alertness is high. If the model predicts that the next episode will be wakefulness, a decision is made as to whether this wake episode will follow the power law distribution, or if it will be a rare "long-wake" episode. To determine if the wake episode will be a "long-wake" episode, a uniform random number is chosen and compared to alertness. If alertness is larger than the random number, the wake episode will be a "long-wake" episode. See details in the Supplemental Material. If the wake episode is not a "long-wake" episode, its duration is calculated as $y*\alpha_W*alertness$ where α_W is a constant scaling factor and y is a random variable generated using the formula given above. If a long-wake episode is initiated, its duration is determined by another random variable uniformly distributed between 5 and 30 min.

Note that SWS episodes durations during baseline were not well fit by an exponential distribution (log-likelihood ratio of −1966.08 vs −1768.05 for Burr See Fig. 3**F**) even though others have found SWS episodes to closely follow an exponential distribution (Lo et al., 2004).

2.4.2. Modeling transitions between sleep states

Once the model has determined the duration of the current episode, it determines which state to transition to next. If the current state is REMS, we found from the baseline data that the next state is roughly equally likely to be SWS or wake, regardless of time of day. Therefore we determine the next state by choosing a uniform random variable between 0 and 1 and set the next state to wake if the random variable is below 0.5 and to SWS if it is not.

During baseline, episodes of SWS are equally likely to transition to wake or REMS early on, but throughout the day, wake becomes more

Table 1
Parameter Values for the homeostatic Process S model used in Fig. 2. The values of the time constants Ti and Td were optimized to minimize the sum of square residuals between the simulation of Process S and delta power during 5-minute episodes of slow-wave sleep. UA and LA represent the upper and lower asymptotes for Process S respectively. UA and LA are not optimized values, but are found using the approach described in Methods. There were no significant differences in the values of LA between baseline and workdays or between Active-work (AW) and Rest-work (RW) groups. The only statistically significant differences in the values of UA (shown in bold) were for the AW group between baseline and workdays ($p = 0.03$) and between AW and RW during the four workdays ($p = 0.007$).

	Baseline				Workdays			
	Ti (optimized)	Td (optimized)	UA	LA	Ti (optimized)	Td (optimized)	UA	LA
AW	12.475 ± 0.598	4.161 ± 0.210	**2.591 ± 0.083**	0.363 ± 0.022	10.748 ± 0.175	2.556 ± 0.047	**3.139 ± 0.206**	0.370 ± 0.042
RW	13.623 ± 0.332	4.418 ± 0.111	2.696 ± 0.138	0.341 ± 0.022	9.654 ± 0.209	2.659±0.147	**2.415 ± 0.122**	0.326 ± 0.026

likely than REMS. Therefore to choose the next state after a SWS episode, we compared a uniformly distributed random variable to a decreasing linear function of time during each 24 h day. If the random variable is less than the linear function, the next state is REMS, if it is more than the linear function, the next state is wake.

If the current state is wakefulness and a rare "long-wake" episode has just happened, the model transitions to SWS. If the wake episode is of usual duration (determined by the power law distribution) the model determines if the next state will be REMS or SWS. Although transitions from wake to REMS are rare in the data (see Tables 3 and 4), they are present. We found that the few wake-to-REMS transitions that did happen in the experimental data tended to happen when sleepiness was very low. Therefore, we made the model transition from wake to REMS only rarely and only if sleepiness is low. Otherwise a wake episode transitions to SWS. For more details of how the model determines bout duration and state transitions, see Supplementary Material.

To our knowledge this is the first model to combine a Markov Chain approach with Processe S and Process C. Since Process S is scaled to be between 0 and 1 and Process C is scaled to be between -0.25 and 0.25, scaling factors were needed to get reasonable values for episode durations and numbers of transitions between states. Since this modeling framework relies on random variables, each simulation is slightly different, similar to how individual recordings are slightly different. Therefore, 50 simulations were run for each figure and average values were plotted along with error bars representing standard error of the mean.

2.4.3. Optimizing parameters

To optimize the fit of the model to the data, we first produced three separate plots of the experimental data for each of the three states: the number of episodes, the episode duration and the percentage of time spent in each state. With five data points per graph (baseline plus four work days) and two groups (AW and RW), this made for a total of $9 \times 5 \times 2 = 90$ data points for matching the model output to the experimental results.

The five model parameters that were varied in order to optimize the fit to the data are the following: Ti (the rising time constant of Process S), Td (the falling time constant of Process S), and three scaling factors: α_W,α_S, and α_R. Since our simple homeostatic model (Fig. 2) predicted a different value of Ti and Td between baseline days and workdays, we first optimized all 5 of the parameters for the baseline day alone both for the AW group and the RW group. This required minimizing the error between the model and the experimental data for 9 data points for each group: number of episodes of each state, episode duration of each state, and percentage of time in each state.

Once optimum values had been determined for the baseline, we next optimized the parameters during the work period by minimizing the differences between the model output and the experimental data for the four workdays. This led to $4 \times 3 \times 3 = 36$ data points for the AW group and another 36 for the RW group that we tuned the model to reproduce as best as possible.

For the optimization of the model during the baseline day we converted the multiobjective problem with 18 objectives (3 sleep measures × 3 sleep states × AW and RW cases) into a single objective problem by taking the average of the Normalized Root Mean Square errors between simulation output and experimental results for all 18 of the data points and then computing an unbiased average of these points. Once the multiobjective optimization problem was turned into a single objective optimization problem, MATLAB's `fminsearch` was used to optimally choose Ti, Td, and the scaling factors to minimize the discrepancy between the model output and the data. The same procedure was carried out to optimize parameter values for the work period except now there were $4 \times 9 \times 2 = 72$ values (4 workdays, 9 measures, AW and RW cases). Again this multiobjective optimization was converted to a single objective optimization by computing an average of the 72 values and then `fminsearch` was used to optimally choose values of Ti, Td, and the scaling factors for the work period.

Note that the parameters used for the rising and declining rates of Process S in the Markov Chain model were optimized and are not the same as those used in the Simple Homeostatic modeling shown in Fig. 2, (note the Ti and Td values in Tables 1 and 2).

Table 2
Optimized parameter values for the Markov Chain simulations. All parameters were optimized separately for the baseline and for the workdays. Simulations for the Active-work (AW) and Rest-work (RW) groups during baseline used the same optimal parameters as we assumed there were no differences in the two groups during baseline. The scaling parameters (αW, αS, and αR) were the same for AW and RW groups, although there were different between the baseline and workdays. The only differences in parameters between the AW and RW groups are the optimal values of the time constants Ti and Td during the work period. Note how for the AW group, Td (but not Ti) becomes smaller during the workdays as compared to baseline. This is consistent with the simpler Process S homeostatic model (Fig. 2). Also, Ti (but not Td) becomes smaller in the work period as compared to the baseline for the RW group. This is also consistent with the results presented in Fig. 2. Ti and Td have units of hours, all the other parameters are dimensionless.

	Baseline					**Workdays**				
	Ti	Td	α_W	α_S	α_R	Ti	Td	α_W	α_S	α_R
AW	17.159	2.180	0.600	1.133	1.100	17.071	1.453	0.700	1.212	1.370
RW	17.159	2.180	0.600	1.133	1.100	15.532	2.254	0.700	1.212	1.370

3. Results

3.1. Homeostatic model

Using the previously described simple homeostatic model (Rempe and Wisor, 2014), Process S was simulated to trace the dynamics of SWA during SWS. By optimizing the choices of the rising time constant (Ti) and the falling time constant (Td), we found that Td values exhibited a significant reduction for both RW ($p < 0.001$) and AW ($p < 0.05$) during the four-day work protocol compared to 24 h baseline while Ti was smaller ($p < 0.001$) during the work protocol only for the RW case (see Fig. 2**A**). Note that compared to human sleep, where sleep is generally consolidated, normal rodent sleep is polyphasic: there are many more transitions between states and episode durations are much shorter. The frequent interruptions of SWS episodes by wake and REMS in rodents may act to decrease the overall decay of Process S as compared to human sleep. On the contrary, longer duration of SWS episodes in RW and AW ($p < 0.001$, both as reported in (Grønli et al., 2017) and shown in Fig. 6**B**) during work compared to baseline may explain the faster decay of sleep pressure indicated by the reduction in Td values. Ti values were also significantly reduced in RW relative to their baseline control values (see Fig. 2**A**), though not in AW. The fact that Ti is not significantly smaller in the AW group during work as compared to baseline indicates that forcing rats to work during their normal active phase may not be sufficient to significantly accelerate the accumulation of sleep need (reflected in changes in Ti). In contrast, forced work during the normal resting phase seems to accelerate the accumulation of sleep need (reflected in a smaller value of Ti compared to baseline). Thus, the model predicts that 8 h forced activity induces changes in the homeostatic behavior; the decay of SWA is faster in both groups during the work period compared to during the 24-hour baseline. The lower asymptote (LA) did not change between the baseline day and the workdays for either the AW or the RW and there were no group differences either (Fig. 2**B**). However, in the AW group, the upper asymptote (UA) was significantly larger during the work days as compared to baseline, and the value of UA during workdays is higher in the AW group than in the RW group. Fig. 2 panels **C** and **D** show one representative run of the simulation for the AW case and the RW case respectively. Table 1 lists optimized values of the time constants Ti and Td during baseline and the work period as well as computed values of UA and LA for each period. These values are similar to those found from other labs (Franken et al., 2001) although larger than we found in an earlier study that did not involve simulated shift work (Rempe and Wisor, 2014). The increase in the upper asymptote in the AW case may compensate for the faster rising of Process S during work as it allows Process S to rise farther than it would ordinarily. The asymptote values did not change significantly between baseline and the work period for the RW group. While this model is helpful in quantifying the time course of SWA during SWS, it does not provide enough detail to model individual sleep episodes.

3.2. Markov chain model

To understand the mechanism behind the differences in episode duration we developed a Markov Chain model of sleep state. As described in the Methods section, the Markov Chain model uses probability to predict the length of time spent in each sleep state and state transitions. To generate a realistic hypnogram, the Markov Chain can be thought of as a sequence of transitions between distinct states where the time spent in the current state and the choice of the next state are determined using random variables. The Markov Chain model produces realistic simulations of rodent sleep with frequent transitions between stages (Fig. 3), both for the AW case (panel **A**) and the RW case (panel **C**). Panels **B** and **D** show 10 h of the same data as shown in panels **A** and **C** respectively. In each panel hypnograms for individual recordings are plotted in the upper portion of the panel and hypnograms for individual runs of the model are plotted in the lower portion of the panel. Individual simulations don't match exactly during baseline because of the randomness built into the model, just as individual recordings from experimental data don't have identical hypnograms during the baseline period. To generate realistic random durations of episodes, we first determined the probability distribution of episode durations found during the baseline period using all subjects in the previous study (Grønli et al., 2017). The durations of wake episodes occurring during the baseline day of the experiment were better fit with a power law than an exponential (Fig. 3**E**), while SWS and REMS episode durations were better fit with a Burr type XII distribution rather than an exponential distribution (Fig. 3 panels **F** and **G** respectively). In each case the blue curve represents the optimized fit of an exponential model to the data. The simulations shown in panels A-D used episode durations generated by random variables whose cumulative probability distributions are shown in panels E, F, and G. During the course of the baseline day, wake episode durations generally became longer (Fig. 3**H**), while SWS episode durations (Fig. 3**I**) and REMS episode durations (Fig. 3**J**) both generally declined.

As shown in Fig. 4, the Markov Chain model replicates the relative probability of each sleep state for both the RW and AW, during baseline and between shifts. Each sleep state has similar percentages compared to the experimental data, including circadian changes.

The values of the optimized parameters for the Markov Chain model, during baseline and during the work days, are shown in Table 2. Both the AW and RW groups have the same set of optimal parameters during baseline and a different set of optimum parameters during the work days. There are no differences in any of the parameters between the AW and RW groups during baseline. Also, there were no differences in the scaling factors between the AW and RW groups during the work days. However, optimal values of the scaling factors were different between baseline and workdays for both groups. The only parameter differences between the simulations for the AW group and the RW group are the values of Ti and Td during the workdays.

We counted the number of transitions between states for each day of simulated data and compared the results to the experimental data. Agreement between the experiments and the simulations is high during the baseline day for both the AW and RW cases. Comparison of the state transition counts in simulated vs. experimental data from the AW condition by Student's T yielded significant differences in the numbers of R-to-W transitions only, during baseline and work day 1 (Table 3). All other types of state transitions occurred at equal frequencies in the real data set and in simulations. However, the agreement of the experimental and simulated data for RW was less than for AW. Comparison of the state transition counts in simulated vs. experimental data from the RW condition by Student's T (Table 4) yielded significant differences in the numbers of SWS-to-Wake, SWS-to-REMS and REMS-to-SWS transitions, though not for any other types of state transitions. In simulated data from RW, SWS-to-Wake transitions were more frequent than in experimental data by roughly 40% on work days 1, 3 and 4. SWS-to-REMS and REMS-to-SWS transitions were less frequent in simulations than experimental data by 25–40% for the RW condition on work days 1 and 2. In both the AW and RW cases the experimental data and the simulations show a similar trend: fewer state transitions during the work days as compared to the baseline day.

The number of episodes in each state across days is well matched by the model (Fig. 5). The experimental data and the simulation output show a significant decrease in the number of wake episodes, SWS episodes and REMS episodes (panels A, B, and C respectively) in all four work days as compared to baseline. While the experimental data show only two differences between AW and RW (SWS episodes on W4 and REMS episodes on W1), the simulation does not show any group differences in the number of episodes. The simulation predicts fewer SWS episodes in W1 and W2 compared to the experimental data for the RW group (panel **B** right side), and fewer REMS episodes for the RW group on each day and fewer REMS episodes for the AW group on the baseline

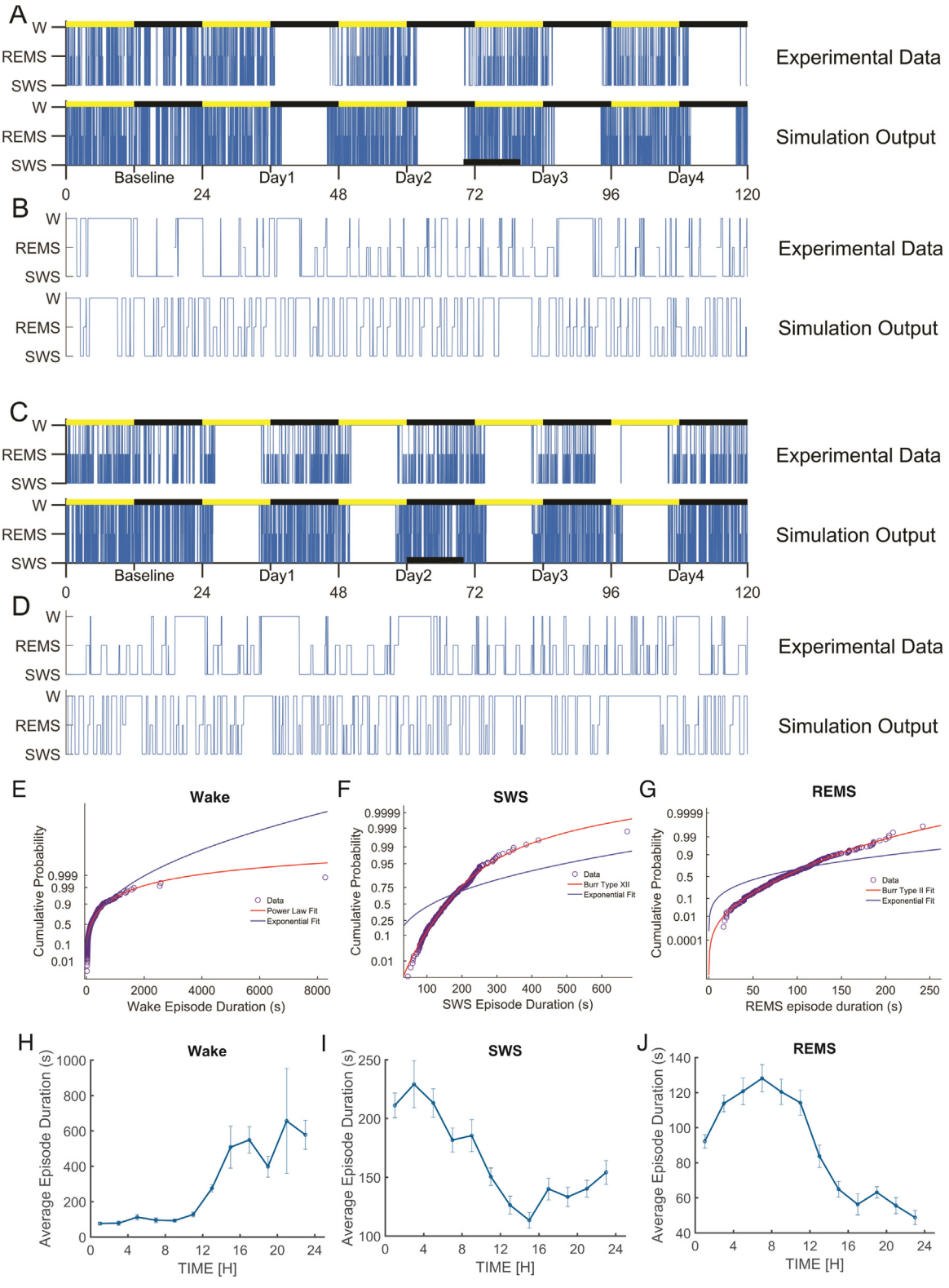

(caption on next page)

day and the first 3 work days (panel **C** right side). Average episode durations for each state (shown in Fig. 6) show similar patterns across the work days and similar group differences in the simulation output as in the experimental data. Specifically, for both SWS and REMS the model correctly reproduces significant increases in episode durations for all work days as compared to baseline. In the case of SWS, the model also replicates significant differences between groups during the work period. For REMS episodes, the model predicts differences between the AW and RW groups although this group difference was not seen in the experimental data. When simulating the AW case the model produces slightly shorter wake episodes during baseline (compared to the experiment) and slightly longer wake episodes on W2, while the RW simulation produces shorter Wake episodes on W4 (panel **A** right side). The model shows much less variation in SWS episode durations than the

Fig. 3. The Markov Chain generates hypnograms that are similar to recorded hypnograms. Shown are individual recordings and individual simulations for active-workers (AW) (**A**) and resting-workers (RW) (**C**) during a 24 h baseline and a 4-day work protocol. The upper row in each panel shows recorded data and the lower panel shows the simulation output. Note the gaps representing work periods starting in the first active phase (ZT14–22) after baseline for the AW group (panel A), and during the first inactive phase (ZT2–10) after baseline for the RW group (panel C). Vertical lines indicate sleep state changes. Yellow and black bars denote times of lights-on and lights-off respectively. Panels **B** and **D** show 10 h of the same data shown in panels **A** and **C.** The black rectangles at the bottom of the simulation output in panels A and C indicate the location of the expanded sections shown in panels B and D respectively. Note the occurrence of long Wake (W) episodes in the recordings and the simulations shown in panels B and D. REMS = rapid eye movement sleep, SWS = slow wave sleep. Panels **E**, **F**, and **G** show the cumulative probability distributions for the durations of Wake, SWS and REMS episodes respectively. Panels E,F,G were generated using experimental data recorded during the baseline. Wake episode durations were better fit with a power law than an exponential (red curve and blue curve respectively), while SWS and REMS episode durations were better fit with a Burr type XII distribution rather than an exponential distribution. In each case the blue curve represents the optimized fit of the exponential model to the data. Panels **H**, **I**, and **J** show changes in episode duration over the course of the baseline day for wake, SWS, and REMS respectively. Data are binned into 2-hour bins. Error bars indicate standard error of the mean.

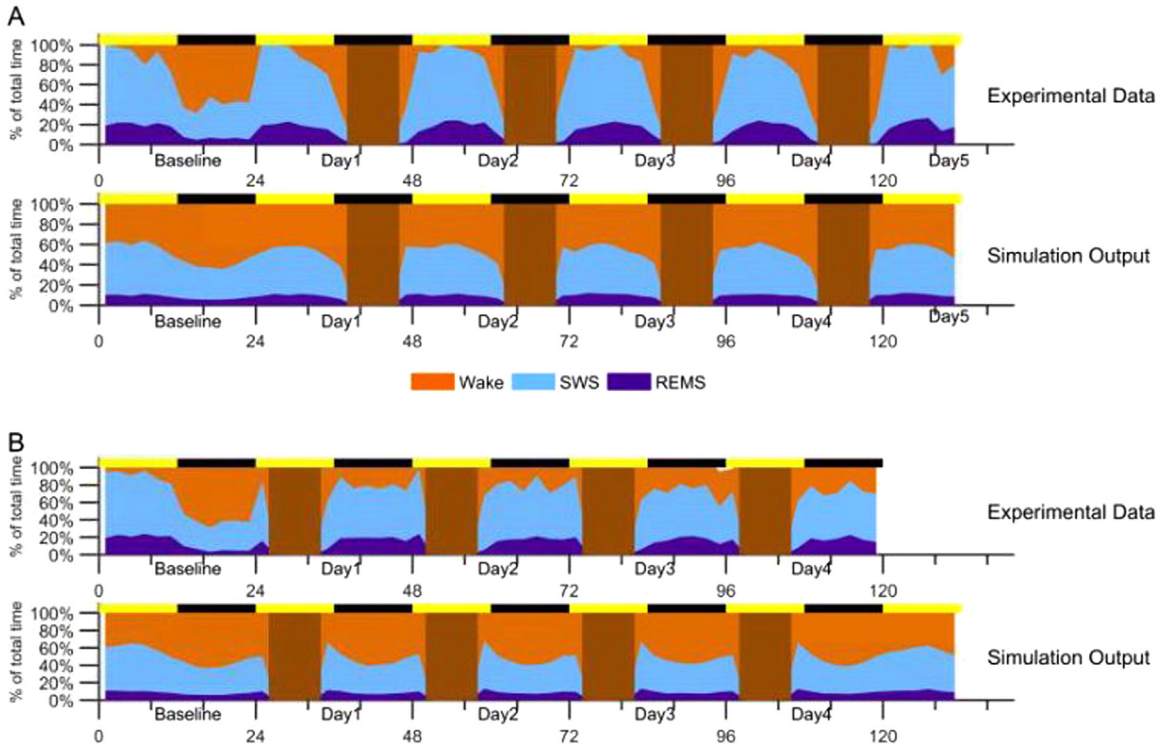

Fig. 4. Sleep/Wake profile of baseline and four work days. Plots of sleep state timing for the Active-workers (AW) (panel **A**) and Rest-workers (RW) (panel **B**) cases. The upper plot in each panel shows the experimentally recorded data and the lower plot shows the output of the model. Alternating yellow and black bands at the top of each panel indicate the timing of light and dark intervals, respectively. Dark brown bands in each panel indicate the time spent in forced ambulation. REMS = rapid eye movement sleep, SWS = slow wave sleep. The upper plots in both panels are reproduced from (Grønli et al. 2017).

Table 3
The number of transitions between states in the active-work case. Each entry contains the mean plus or minus the standard deviation of numbers of each type of transition in each day. Note the close agreement between data and simulation in the baseline day and similar trends between experimental data and simulation output over the days of the experiments. W = workdays 1 to 4, SWS = slow wave sleep, REMS = rapid eye movement sleep. Asterisks indicate significant Bonferroni corrected T tests for simulation vs analogous experimental data.

	Baseline	W1	W2	W3	W4
Wake - > SWS (data)	182.92 ± 13.74	129.00 ± 9.27	104.08 ± 8.89	104.67 ± 9.22	96.67 ± 13.04
Wake - > SWS (simulation)	180.08 ± 2.95	111.42 ± 1.49	108.50 ± 2.09	106.75 ± 2.03	107.67 ± 2.96
Wake - > REMS (data)	6.92 ± 3.39	3.00 ± 1.33	2.25 ± 1.18	3.58 ± 2.33	3.50 ± 1.36
Wake - > REMS (simulation)	2.17 ± 0.42	2.00 ± 0.25	3.42 ± 0.38	2.25 ± 0.35	2.75 ± 0.52
SWS - > Wake (data)	130.25 ± 10.06	92.33 ± 6.91	73.25 ± 4.97	76.33 ± 6.55	68.67 ± 8.96
SWS - > Wake (simulation)	142.67 ± 2.76	90.33 ± 2.27	88.08 ± 1.83	87.25 ± 1.53	86.58 ± 2.55
SWS - > REMS (data)	79.92 ± 8.03	59.58 ± 4.67	51.75 ± 4.79	50.42 ± 4.20	43.83 ± 6.27
SWS - > REMS (simulation)	79.42 ± 2.73	46.25 ± 1.94	44.75 ± 1.93	43.00 ± 1.78	45.75 ± 1.12
REMS - > Wake (data)	57.92 ± 5.99	39.33 ± 5.13	32.17 ± 5.37	30.75 ± 5.03	30.00 ± 5.44
REMS - > Wake (simulation)	39.92 ± 1.59*	23.17 ± 1.57*	23.67 ± 1.38	21.83 ± 1.42	23.83 ± 1.11
REMS - > SWS (data)	40.75 ± 7.35	30.50 ± 4.86	30.75 ± 4.05	31.75 ± 4.02	29.08 ± 5.19
REMS - > SWS (simulation)	41.42 ± 2.43	25.33 ± 1.45	24.33 ± 1.31	23.50 ± 1.26	24.67 ± 0.95

Table 4
The number of transitions between states in the rest-work case. Each entry contains the mean plus or minus the standard deviation of numbers of each type of transition in each day. Note the close agreement between data and simulation in the baseline day and similar trends between experimental data and simulation output over the days of the experiments. W = workdays 1 to 4, SWS = slow wave sleep, REMS = rapid eye movement sleep. Values are presented as mean ± standard deviation. Asterisks indicate significant Bonferroni corrected T tests for simulation vs analogous experimental data.

	Baseline	W1	W2	W3	W4
Wake - > SWS (data)	170.60 ± 11.05	98.40 ± 8.82	106.93 ± 11.21	94.93 ± 7.05	97.87 ± 7.81
Wake - > SWS (simulation)	183.07 ± 2.49	109.40 ± 1.95	108.93 ± 2.47	110.47 ± 1.81	109.27 ± 1.82
Wake - > REMS (data)	3.67 ± 1.01	2.93 ± 0.92	3.47 ± 1.27	3.60 ± 1.63	3.80 ± 1.13
Wake - > REMS (simulation)	3.13 ± 0.47	2.20 ± 0.35	2.67 ± 0.41	2.40 ± 0.36	2.47 ± 0.27
SWS - > Wake (data)	122.40 ± 9.13	63.33 ± 5.68	74.20 ± 8.41	62.20 ± 3.40	62.40 ± 3.83
SWS - > Wake (simulation)	147.13 ± 2.65	87.27 ± 1.87*	86.93 ± 2.25	89.13 ± 1.88*	87.47 ± 1.81*
SWS - > R (data)	87.80 ± 6.69	67.40 ± 4.80	58.80 ± 3.05	51.00 ± 4.11	52.00 ± 4.48
SWS - > R (simulation)	75.80 ± 1.72	45.53 ± 1.36*	43.73 ± 1.10*	44.87 ± 1.47	46.53 ± 2.11
R - > Wake (data)	49.87 ± 4.27	36.07 ± 5.05	33.13 ± 4.81	31.47 ± 4.85	33.80 ± 4.67
R - > Wake (simulation)	39.67 ± 1.22	24.13 ± 1.11	24.47 ± 0.93	23.87 ± 1.00	24.13 ± 1.42
R - > SWS (data)	50.33 ± 7.51	41.13 ± 5.08	37.47 ± 4.55	34.40 ± 3.98	36.00 ± 4.31
R - > SWS (simulation)	39.27 ± 1.12	23.53 ± 1.15*	21.93 ± 1.15*	23.27 ± 1.35	24.87 ± 1.15

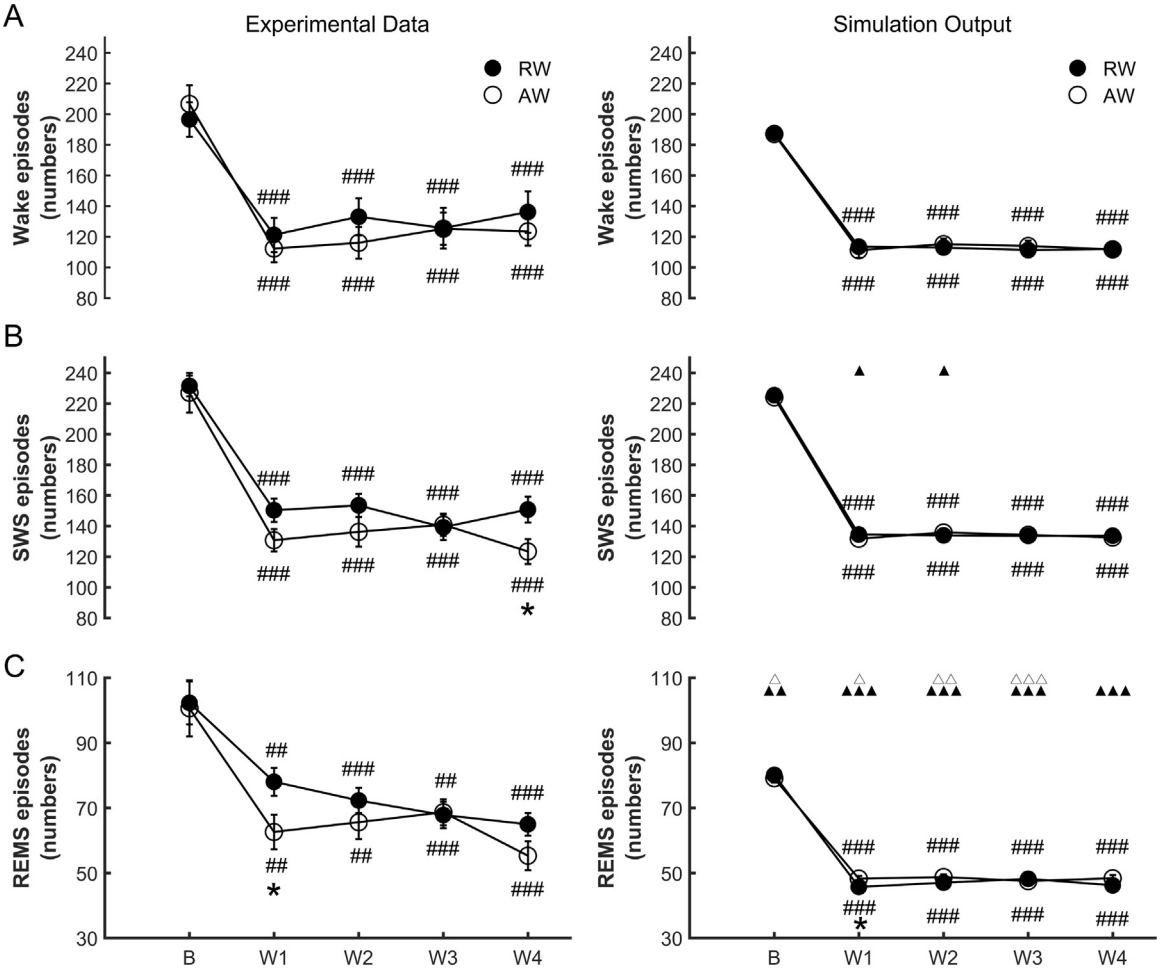

Fig. 5. Comparison of Experimental Data to model output: numbers of episodes of each state. In the experimental data (left panels) both the Active-work (AW) and Rest-work (RW) groups showed fewer wake episodes (upper left panel), fewer slow-wave sleep (SWS) episodes (middle left panel), and fewer rapid eye movement sleep (REMS) episodes (lower left panel) between workdays (W1 to W4) as compared to baseline, with no difference between the two groups except SWS episodes on W4 and REMS episodes on W1. The simulation output (right column) showed very similar numbers of episodes of each state and the same statistical differences between baseline and workdays. Only REMS episodes on W1 showed a significant difference between AW and RW. Error bars in the simulation panels represent SEM from 50 simulations. Asterisks in all panels indicate significant differences between RW (n = 15 in experimental data) and AW (n = 12 in experimental data); * $p < 0.05$, ** $p < 0.01$, *** $p < 0.001$, and hashes denote significant differences compared to baseline: # $p < 0.05$, ## $p < 0.01$ and ### $p < 0.001$. When AW and RW data points overlay, asterisks above the data point refer to RW and asterisks below the data refer to AW. Open and filled triangles above graphs in right hand panels represent significant differences compared to experimental data for the AW and RW groups respectively. One triangle: $p < 0.05$, two triangles: $p < 0.01$, three triangles: $p < 0.001$.

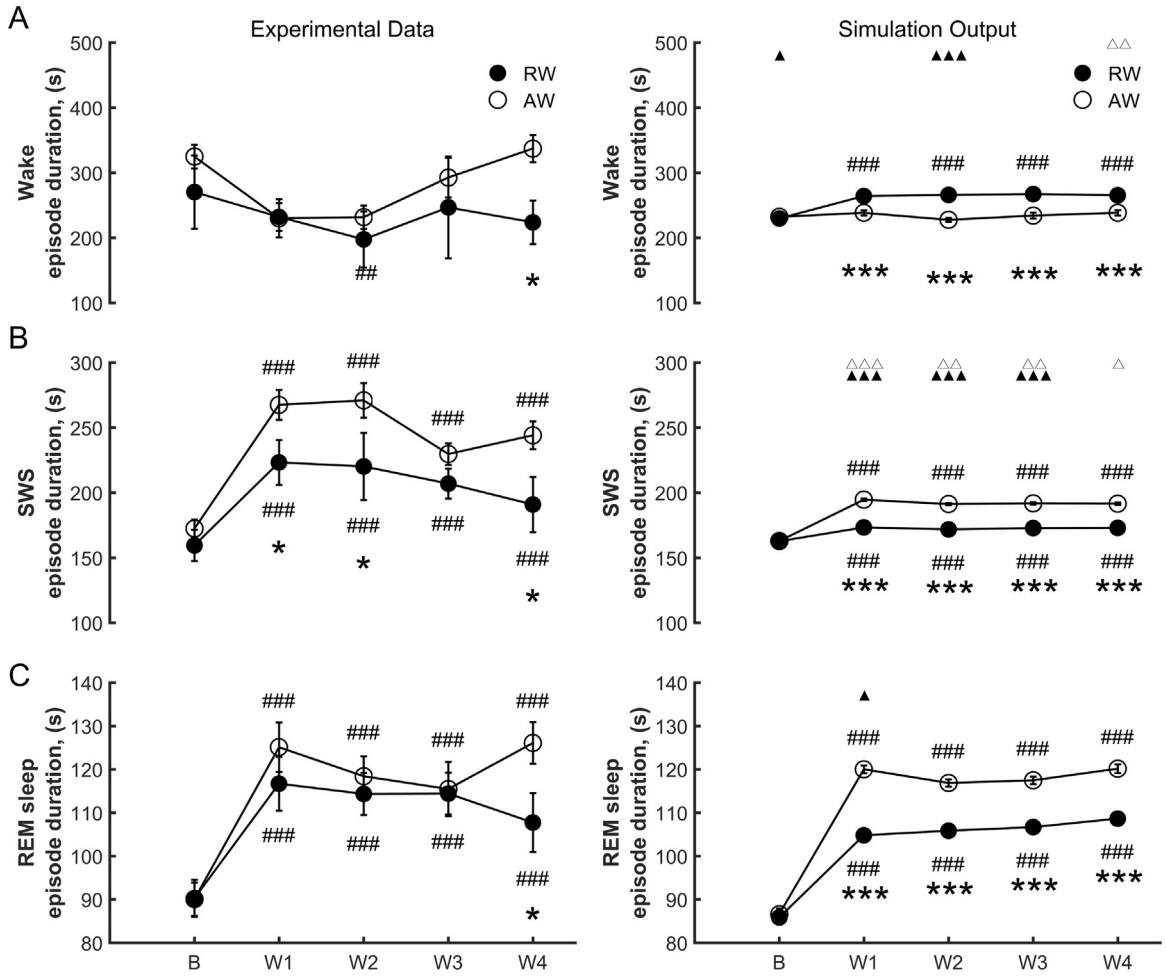

Fig. 6. Comparison of Experimental Data to Model Output: Episode Duration. A In the experimental data (left panel), Wake episode durations changed only slightly with no significant difference between baseline (B) and workdays (W1 to W4) except Rest-work (RW) at W2 which was significantly lower than baseline. There was no significant difference between RW and Active-work (AW) until W4. In the simulation output (right panel), wake episode durations were similar to those in the experimental data, but the RW group changed slightly from baseline in all four workdays and there was a small but significant difference between work groups for each of the work days. **B** In the experimental data, both groups showed an increase in slow-wave sleep (SWS) episode duration between workdays as compared to baseline (left panel), with the AW group experiencing longer durations compared to the RW group. Significant differences between baseline and workdays and between AW and RW was captured with the mathematical model (right panel). **C** In the experimental data (left panel) REM sleep episodes became significantly longer between workdays as compared to baseline with no difference between AW and RW until W4. In the simulations the differences between baseline and workdays was captured accurately, although a difference between AW and RW was introduced. Error bars in the simulation panels represent SEM from 50 simulations. Asterisks in all panels indicate significant differences between RW (n = 15 in experimental data) and AW (n = 12 in experimental data); * $p < 0.05$, ** $p < 0.01$, ***$p < 0.001$, and hashes denote significant differences compared to baseline: # $p < 0.05$, ## $p < 0.01$ and ### $p < 0.001$. Open and filled triangles above graphs in right hand panels represent significant differences compared to experimental data for the AW and RW groups respectively. One triangle: $p < 0.05$, two triangles: $p < 0.01$, three triangles: $p < 0.001$.

experimental data do, and it generates SWS episodes that are shorter than those in the experimental data for workdays 1 through 3 for both groups and also on W4 for the AW group (panel **B** right side). The simulation matches REMS episode durations for both groups on each day except W1 when REMS durations are too short for the RW case (panel **C** right side).

The experimental data show that the percentage of time spent in wakefulness rises modestly yet significantly during the workdays as compared to the baseline day for both AW and RW groups. On workdays 1 and 3 the RW group shows a slightly higher percentage of time spent in wakefulness as compared to the AW group, while on workday 4 it shows a slightly lower percentage compared to AW (Fig. 7**A** left panel). The simulation output reproduces a modest yet significant increase in the percentage of time spent in wakefulness as compared to baseline for the RW group, but not for the AW group. The model predicts a significant decline for the AW group compared to baseline, but a significantly larger portion of time spent in wake during all four work days for the RW group as compared to the AW group (Fig. 7**A** right panel). Compared to the experimental data, the simulation predicted more time in wakefulness during the baseline and less for each workday for the AW group. On days W1, W3, and W4 the model predicts a significantly lower percentage of time in Wakefulness. The experimental data exhibit a significant decline in the percentage of SWS as compared to baseline in all four work days in both AW and RW groups and significantly more time spent in SWS for the AW group as compared to the RW group during workdays 2 through 4 (Fig. 7**B** left panel). The model also shows a significant decline in SWS percentage during the work week as compared to baseline in the RW group but not the AW group and a higher percentage of SWS in the AW group as compared to the RW group for all four work days (Fig. 7**B** right panel). While the simulation correctly predicts the SWS percentage of the baseline day, both the AW group and the RW group are higher than the experimental data for each work day. Both the experimental data (Fig. 7**C** left panel) and the simulation (Fig. 7**C** right panel) show that REMS comprises

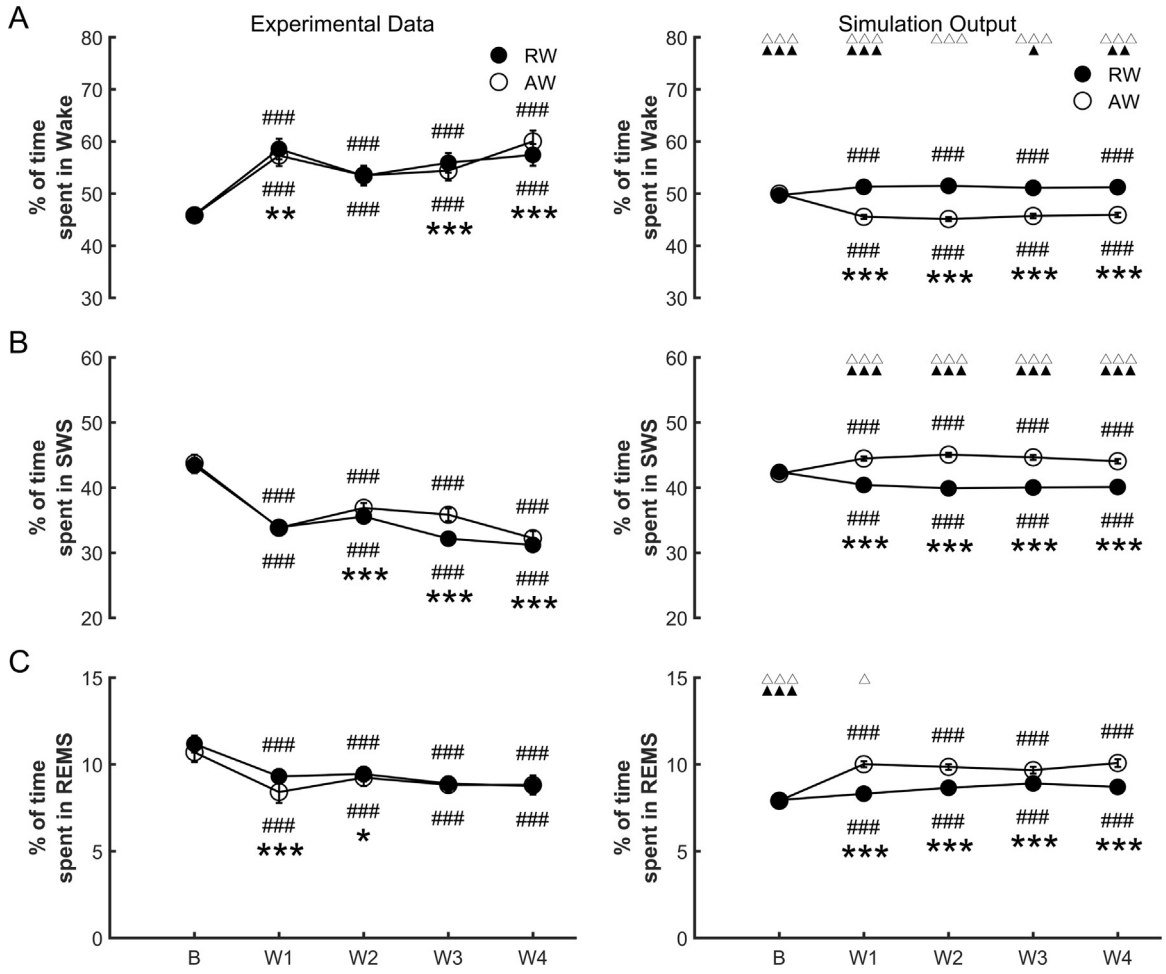

Fig. 7. Comparison of Experimental Data to Model Output: Percentage of time spent in each state. A In the experimental data (left panel), the percentage of time spent in wakefulness (over each workday, W) increases modestly but significantly in both Active-work (AW) and Rest-work (RW) groups compared to baseline (B). The experimental data showed a significant drop in the percentage of time spent in slow-wave sleep (SWS) as compared to baseline for both groups (**B** left panel) and a lower percentage of time in SWS for the RW group on days W2, W3, and W4. The simulation reproduced the significant drop in the RW group, but not the AW group and the model demonstrates a significantly longer SWS episodes for all four work days, rather than the W2-W4. The experimental data showed modest yet significant drop in time spent in rapid eye movement sleep (REMS) for both AW and RW groups as compared to baseline with AW showing a significantly lower value than RW on days W1 and W2. In the simulation RW was significantly lower than AW for all four work days while both groups showed a slight increase with respect to the baseline value. Asterisks in all panels indicate significant differences between RW ($n = 15$ in experimental data) and AW ($n = 12$ in experimental data); * $p < 0.05$, ** $p < 0.01$, ***$p < 0.001$, and hashes denote significant differences compared to baseline: # $p < 0.05$, ## $p < 0.01$ and ### $p < 0.001$. When AW and RW data points overlay, asterisks above the data point refer to RW and asterisks below the data refer to AW. Open and filled triangles above graphs in right hand panels represent significant differences compared to experimental data for the AW and RW groups respectively. One triangle: $p < 0.05$, two triangles: $p < 0.01$, three triangles: $p < 0.001$.

about 10% of the baseline day and changes during the work week are small (a decrease in the experimental data and a small increase in the simulation output). In the experimental data the AW group showed a slightly lower percentage of REMS compared to the RW case for days W1 and W2, while the simulation showed slightly higher percentage of REMS throughout the four work days. The model prediction was not significantly different compared to experimental data except for the baseline day where it predicted too little REMS in each group and W1 where it predicted too much REMS for the AW group only. Compared to the corresponding data in Figs. 5 and 6, the experimental data in Fig. 7 show little variation from animal to animal, which may explain why some differences between the simulation and the experimental data are significant even though they are small.

The modeling framework allows us to monitor the time course of individual variables like the homeostat. While the homeostat begins at nearly the same point at the end of a work shift in the AW and RW case, it does not fall as low for RW between shifts as it does for AW (Fig. 8**A**). This is because alertness is quite high between shifts in the RW case (Fig. 8**B**), which leads to more wakefulness and therefore sleep pressure is not alleviated as much between shifts. Alertness is higher between shifts in the RW case because alertness depends on the circadian rhythm (Process C), which is higher between shifts for the RW group than for the AW group.

The Markov Chain simulation suggests that SWS episodes are shorter for the RW than AW due primarily to the circadian modulation of state transition probabilities. Specifically, Fig. 8**B** illustrates that although sleepiness is very high right after work for the RW, it quickly decreases as a result of increasing circadian alertness. Lower overall sleepiness between shifts leads to shorter SWS episodes as compared to the AW group.

4. Discussion

Knowing that simulated shift work makes a significant impact on sleep architecture during a 4-day shift work protocol, the aims of the current study were: 1) to quantify differences between baseline and

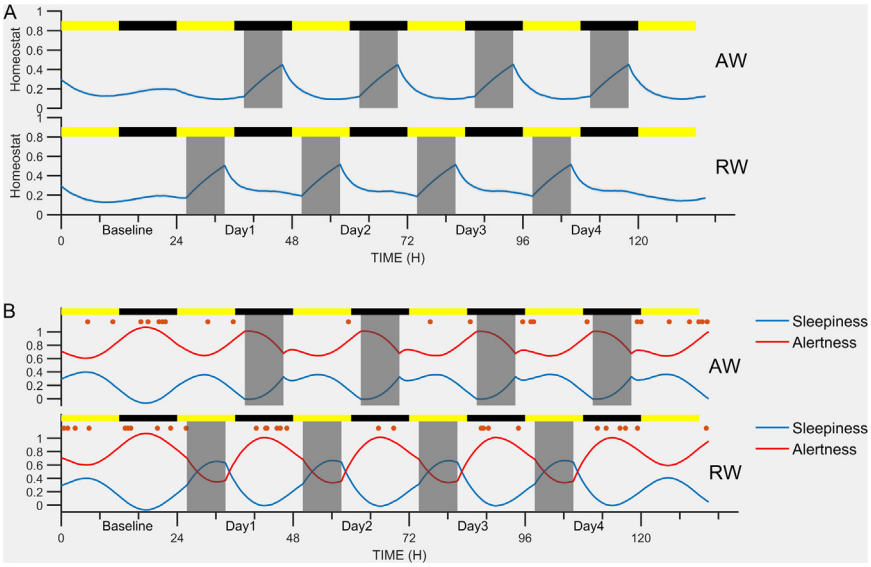

Fig. 8. Homeostat, sleepiness, and alertness in simulations. A The simulated homeostat for both groups (upper panel: Active-work, AW; lower panel: Rest-work, RW) Shown in the average homeostat value for each epoch averaged over 50 simulations. **B** Sleepiness (blue curves) and Alertness (red curves) for both groups (upper panel: AW, lower panel: RW). Shown are average values, averaged over 50 simulations. In all panels, yellow and black bars represent times of lights-on and lights-off respectively. Vertical gray bands represent work shifts. Long-wake episodes (indicated with red dots in panel **B**) tend to happen when sleepiness is low. Long-wake episodes are less common than regular wake episodes and tend to happen when alertness is high.

work day slow wave dynamics for shift-workers and non shift workers, and 2) illuminate possible mechanisms underlying changes in sleep architecture induced by the shift work protocol. This includes changes during the work period as compared to baseline and differences between groups during the work period. For the first aim, we quantified the rising and falling rates of Process S for both the AW group and the RW group during the 24 h baseline and the 4-day shift schedule. We found that for both groups the time constant of the decay of Process S during SWS is faster during the work week than during baseline, and Process S also rises significantly faster during the workdays for the RW group but not significantly so for the AW group.

For the second aim of the study we developed a hybrid model of sleep in rodents that correctly predicts durations of individual sleep states at all circadian phases. This model correctly reproduces the sleep structure of the AW subjects and the RW subjects during both the baseline and the work period. Specifically, it correctly reproduces percentages of time spent in each state throughout the baseline day plus the four days of the simulated shift work. It also correctly reproduces many features of the sleep structure: the number of episodes of each state, episode durations, and the percentage of time spent in each state. Importantly, this mathematical model suggests that some of the differences between sleep in the AW group and RW group can be explained by the circadian rhythm since the RW subjects are trying to sleep when their circadian drive to sleep is low.

4.1. Homeostatic model

Using a simple homeostatic model, we found that although both of the time constants differed between the baseline day and the work days for the rest-workers, there were no significant differences in either of the time constants between the rest-workers and active-workers. Hence, this simple modeling framework seems to suggest that although working alters the time course of homeostatic processes (as compared to baseline), differences in the circadian timing of work does not seem to fundamentally change Process S. This underscores the fact that Process S is time- (hours being awake) and use- (level of activity) dependent, and not circadian (time-of day being awake) dependent. This is consistent with the standard interpretation of the two-process model: that Process S and Process C act independently of one another. Recent reports on the two-process model have suggested that Process S and Process C are probably not truly independent, but are likely subject to more complex interactions (van Diepen et al., 2014). Incorporating this type of interaction between Processe S and Process C may help future models corroborate experimental data even better.

The immediate effects of night-shift work (including a reduction in alertness and performance on duty and changes in sleep architecture during sleep after work) could not be explained by a model that only includes a homeostatic component. One of the more curious experimental results observed after simulated shift work in rats were that SWS episodes occurring in the 16-hr interval between the work shifts were shorter for the rest-workers than for the active-workers. This result could in fact explain the immediate effects of night-shift work and was one of the main motivations to construct and analyze a mathematical model that could incorporate switches between the states. To simulate individual SWS episodes we developed a Markov Chain model.

4.2. Markov chain model

A Markov Chain framework is a good choice for modeling sleep architecture since each episode duration or state transition is impossible to predict exactly, but we can say that some outcomes are more likely than others based on alertness and sleepiness (which account for time of day, and recent sleep history). Each experimental recording is different than other recordings in terms of sleep metrics like average episode durations and the numbers of state transitions, but there tend to be patterns. In the Markov Chain model we hope to capture these overall patterns as well as generate realistic individual recordings. Also, note that although the state transitions are random, they are not uniformly random. That is to say, not each state transition is equally likely at any one time, but model is biased toward some transitions rather than others. For example, if the current state of the model is SWS and alertness is high the model is more likely to transition to REMS rather than wake.

Several research groups have previously used models based on Markov Chains to simulate sleep state transitions in human sleep (Bianchi et al., 2012; Bizzotto et al., 2010; Kemp and Kamphuisen, 1986; Kjellsson et al., 2011; Yang and Hursch, 1973; Yassouridis et al., 1999; Zung et al., 1965) and in rodents (Bari et al., 1981; Kostyalik et al., 2014).

Although the idea of a mathematical model where episode durations depend directly on sleepiness and alertness is novel, there is experimental data to support the idea that episode duration is a function of

circadian time, at least in mice (Easton et al., 2004). Although some previous studies, (Kemp and Kamphuisen, 1986) have included dependence on clock time or other measures to describe some aspects of the simulated sleep structure, to our knowledge our model is the first to model rodent sleep, predicting episode durations using sleepiness and alertness as inputs. Bari et al. (Bari et al., 1981) used sleep state transition functions to quantify aspects of rodent sleep like bout durations, but did not use the model to generate realistic hypnograms. Kostyalik et al. (Kostyalik et al., 2014) used a similar Markov Chain approach to investigate the effects of escitalopram and REMS deprivation on the transition rates between sleep states. However, they assumed that the transition rates were essentially constant during an onset phase and then again during a steady phase.

Whereas it was equally effective in predicting time spent in sleep states for both AW and RW, modeling was not equally effective in predicting state transition counts across the two groups. The prediction of state transition frequency was better for AW (Table 3) than RW (Table 4). Since model fitting was equally effective in predicting state transitions in baseline, yielding no significant differences between simulations and data in both AW and RW, the significant differences between simulation and data that emerged on working days does appear to be an effect of the experimental manipulation. In this sense, the model does not fully convey the basis for sleep disruption by RW. The model emphasizes the interactions of the brain's circadian clock and its sleep homeostat. What additional process might influence sleep in a shift work paradigm? The obligatory use of skeletal muscle during the circadian resting phase might impact systemic sleep regulatory factors. Skeletal muscle upon exertion, releases hormones ('myokines' including interleukin 6, interleukin 8 and brain-derived neurotrophic factor (Pratesi, 2013)). Circulating levels of interleukin 6 and interleukin 8 (Altara et al., 2015), and those of brain-derived neurotrophic factor (Begliuomini et al., 2008) exhibit circadian fluctuations. Since interleukin 6 (Morrow and Opp, 2005), interleukin 8 (García-García et al., 2004) and brain-derived neurotrophic factor (Bachmann et al., 2012) have all been shown to impact sleep, it is possible that the perturbation of circulating myokines by enforced use of skeletal muscle in the resting phase influences sleep. This factor is neither measured nor modeled independently of the brain's endogenous circadian and homeostatic processes in the current study, and may thus limit the predictive utility of the current model, rendering it less effective in predicting sleep in RW rats than AW rats.

The Markov Chain model identifies mathematical parameter values that simulate the duration of time that the individual will remain in a given state before transitioning into another state. By using this model, the present study suggests a putative mechanism behind the sleep differences between the two types of simulated shift work. In the model the length of SWS episodes depends on sleepiness. Consequently, exposure to enforced ambulation for 8 h per day at the time of day when the animal is primed for sleep forced subjects to recover sleep during the endogenous active phase when Process C is high (and therefore alertness is high and sleepiness is relatively low). This increase in alertness (and decrease in sleepiness) meant that SWS episodes were shorter as compared to the active-workers that sleep in-phase with their circadian drive for sleep.

The Markov Chain simulation suggests that SWS episodes are shorter for the rest-workers than active-workers due primarily to the circadian modulation of state transition probabilities. Specifically, Fig. 8**B** illustrates that although sleepiness is very high right after work for the rest-workers, it quickly drops, not as a result of the homeostat dropping, which is blunted in these animals compared to AW, but rather due to the circadian rhythm. Lower overall sleepiness between shifts leads to shorter SWS episodes as compared to the AW group.

These results may imply that the degraded wake functioning observed in both humans and animals, and in both field and laboratory studies related to shift work, may derive primarily from the circadian component. This vulnerability may not only be due to sleep loss, but rather due to a mismatch between work demands and the brain's ability to overcome the circadian challenges imposed by night-shift work. Future animal and modeling studies should combine simulated shift work with recovery in constant darkness, allowing study of the free-running endogenous circadian rhythm, to further elucidate the possible circadian mechanisms.

In our Markov Chain model the frequency distribution of episode durations is skewed, not normal: episodes of any sleep state are more likely to be short than long. This assumption is supported by experimental data that show that in rats under normal conditions short bout durations are more common than long ones (Trachsel et al., 1991). However, that same study showed that after sleep deprivation, medium-length SWS episodes become more frequent than short episodes (Trachsel et al., 1991). Further refinements of the model may therefore benefit from a more complicated distribution function that changes as a function of sleep need.

In the Markov Chain simulations, the optimum value for Ti does not change between baseline and workdays for the AW group, but for the RW group the optimum value of Ti changes from 17 h in the baseline to 15.5 h during workdays. This is very consistent with what we found using the simple Process S model: rest-workers had a significant change in Ti from baseline to workdays (13.6 to 9.6 to about 9) while the active-workers did not (see Tables 1 and 2 and Fig. 2). The time constant of the falling of Process S (Td) did not decrease during the work period as compared to the baseline for the RW group, but it did decrease for the AW group.

Note that the Markov Chain simulations for the active-workers and the rest-workers use the same equations and parameter values except for Ti and Td during the work period. Otherwise the only difference between the two simulations is the schedule of when wakefulness is enforced. By using such a simple model and only changing two variables between AW simulations and RW simulations we hope to demonstrate that some of the experimental differences seen between the two groups can be explained by interactions of a homeostat and a circadian rhythm in the context of enforced wakefulness, rather than by a more complicated model with many numerical parameters.

4.3. Developing a mathematical model of rodent sleep

One of our goals in developing a mathematical model for rodent sleep was to be consistent with the two-process model formulation, since the two-process model is a ubiquitous framework for modeling the timing of sleep, although in its most basic form it has been used primarily to model human sleep. One of the original two-process model papers (Daan et al., 1984) demonstrated that the basic model can simulate polyphasic rodent sleep by setting the two C curves close to each other so the curve for Process S changes direction more frequently. However, while this approach does yield shorter episodes as compared to human sleep, in the present study this formulation did not yield episode durations or circadian dependence concordant with empirical rodent data (data not shown). Since one of our requirements was to closely match episode duration in empirical data, we pursued another approach.

Some groups (Franken et al., 2001, 1991; Vyazovskiy and Tobler, 2012; Vyazovskiy et al., 2007) have used parts of the two-process model for rodent sleep, although with a different approach. In those papers, Process S is used to quantify the time course of the rising and falling of SWA as measured during SWS. However, Process C is not used directly in these models. In the present study our approach is opposite: instead of starting with the sleep/wake information about the rodent and using that to optimize Process S relative to empirical SWA data, we are trying to use Process S (along with Process C) to *predict* the time course over which the rodent will transition from sleep to wake or vice versa. In this sense, both the purpose and outcome of the current mathematical model of rodent sleep are unique.

Although the current models do not model the effect of light, a

further elaboration of these models may account mathematically for effects of light/dark cycles on Process C, similar to what was used in previous models (Postnova et al., 2012; St Hilaire et al., 2007) or alterations of Process C due to shift work since several studies have shown that shift work alters many circadian rhythms (Marti et al., 2016; Salgado-Delgado et al., 2008). Sleep deprivation reduces SCN neuronal activity response to light, indicating that circadian rhythms may be affected by sleep homeostatic pressure (van Diepen et al., 2014). By working and hence being awake with eyes open at a time when they are usually inactive, the RW group was also receiving more light than they would normally during that period. This change in light input (along with the enforced wakefulness) may have a significant effect and future models that account for light will be able to take this into account. Here we have endeavored to use models that are as simple as possible to explain the phenomena at hand and by using models that do not include the effects of light directly, we have fewer parameters. Since we were able to reproduce nearly all of the significant experimental results in the sleep structure shown in the experimental data with our current Markov Chain model that does not include the effect of light on the circadian rhythm, we propose that this additional component may only make a modest improvement in the agreement of the model with the experimental data. Our results suggest that although the change of light input due to shift work may play a significant role in the sleep architecture of each group, it is likely to make a smaller influence than working at the wrong circadian phase. We expect that including the phase-shifting effects of light may further extend our results and further improve the fit of the models to the data.

5. Conclusions

We constructed and analyzed a simple mathematical model of rodent sleep to understand mechanisms underlying experimental results of a rodent shift work protocol. To our knowledge this model of rodent sleep is unique in that it is consistent with the two-process model, and it predicts precise sleep architecture based on Process C, Process S, and external manipulations like enforced wakefulness. Additionally, our model makes use of a Markov Chain to determine episode durations and transitions between sleep states. Since the model reproduces some key features of the experimental data, it can be used to examine possible mechanisms underlying sleep differences between active-workers and rest-workers. Specifically, our model predicts that shorter SWS episodes in rest-workers between shifts is primarily a circadian effect. Since these subjects show a stronger circadian drive for wakefulness between shifts, they tend to have shorter SWS episodes. The model used is simple and requires few assumptions. It was not necessary to change Process C, the rate of change of Process S, or any of the scaling factors between the two groups. It is our hope that this modeling framework will open up further avenues of investigation across different experimental manipulations of sleep/wake cycles.

Conflict of interest

The authors declare there are no conflicts of interest associated with this publication.

Appendix A. Supporting information

Supplementary data associated with this article can be found in the online version at http://dx.doi.org/10.1016/j.nbscr.2018.04.002.

References

Achermann, P., Borbély, A.A., 1994. Simulation of daytime vigilance by the additive interaction of a homeostatic and a circadian process. Biol. Cybern. 71 (2), 115–121.

Akerstedt, T., Torsvall, L., Gillberg, M., 1987. Sleepiness in shiftwork. A review with emphasis on continuous monitoring of EEG and EOG. Chrono-. Int. 4 (2), 129–140.

Akerstedt, T., Wright Jr., K.P., 2009. Sleep loss and fatigue in shift work and shift work disorder. Sleep Med. Clin. 4 (2), 257–271.

Altara, R., Manca, M., Hermans, K.C.M., Daskalopoulos, E.P., Brunner-La Rocca, H.-P., Hermans, R.J.J., Blankesteijn, M.W., 2015. Diurnal rhythms of serum and plasma cytokine profiles in healthy elderly individuals assessed using membrane based multiplexed immunoassay. J. Transl. Med. 13, 129.

Arble, D.M., Bass, J., Behn, C.D., Butler, M.P., Challet, E., Czeisler, C., Wright, K.P., 2015. Impact of sleep and circadian disruption on energy balance and diabetes: a summary of workshop discussions. Sleep 38 (12), 1849–1860.

Bachmann, V., Klein, C., Bodenmann, S., Schäfer, N., Berger, W., Brugger, P., Landolt, H.-P., 2012. The BDNF Val66Met polymorphism modulates sleep intensity: EEG frequency- and state-specificity. Sleep 35 (3), 335–344.

Bari, F., Rubicsek, G., Benedek, G., Obál Jr, F., Obál, F., 1981. Analysis of ultradian sleep rhythms in rats, using stage transition functions. Electroencephalogr. Clin. Neurophysiol. 52 (4), 382–385.

Begliuomini, S., Lenzi, E., Ninni, F., Casarosa, E., Merlini, S., Pluchino, N., Genazzani, A.R., 2008. Plasma brain-derived neurotrophic factor daily variations in men: correlation with cortisol circadian rhythm. J. Endocrinol. 197 (2), 429–435.

Bianchi, M.T., Eiseman, N.A., Cash, S.S., Mietus, J., Peng, C.-K., Thomas, R.J., 2012. Probabilistic sleep architecture models in patients with and without sleep apnea. J. Sleep. Res. 21 (3), 330–341.

Bizzotto, R., Zamuner, S., De Nicolao, G., Karlsson, M.O., Gomeni, R., 2010. Multinomial logistic estimation of Markov-chain models for modeling sleep architecture in primary insomnia patients. J. Pharmacokinet. Pharmacodyn. 37 (2), 137–155.

Borbély, A.A., Achermann, P., 1992. Concepts and models of sleep regulation: an overview. J. Sleep Res. 1 (2), 63–79.

Borbély, A., Daan, S., Wirz-Justice, A., Deboer, T., 2016. The two-process model of sleep regulation: a reappraisal. J. Sleep Res. 25 (2), 131–143.

Daan, S., Beersma, D.G., Borbély, A.A., 1984. Timing of human sleep: recovery process gated by a circadian pacemaker. Am. J. Physiol. 246 (2 Pt 2), R161–R183.

Dijk, D.J., Beersma, D.G., Daan, S., 1987. EEG power density during nap sleep: reflection of an hourglass measuring the duration of prior wakefulness. J. Biol. Rhythm. 2 (3), 207–219.

Doran, S.M., Van Dongen, H.P., Dinges, D.F., 2001. Sustained attention performance during sleep deprivation: evidence of state instability. Arch. Ital. De. Biol. 139 (3), 253–267.

Easton, A., Meerlo, P., Bergmann, B., Turek, F.W., 2004. The suprachiasmatic nucleus regulates sleep timing and amount in mice. Sleep 27 (7), 1307–1318.

Edgar, D.M., Dement, W.C., Fuller, C.A., 1993. Effect of SCN lesions on sleep in squirrel monkeys: evidence for opponent processes in sleep-wake regulation. J. Neurosci.: Off. J. Soc. Neurosci. 13 (3), 1065–1079.

Folkard, S., Akerstedt, T., 1989. Towards the Prediction of Alertness on Abnormal Sleep/Wake Schedules. In *Vigilance and Performance in Automatized Systems/Vigilance et Performance de l'Homme dans les Systèmes Automatisés*, pp. 287–296.

Folkard, S., Tucker, P., 2003. Shift work, safety and productivity. Occup. Med. 53 (2), 95–101.

Franken, P., Chollet, D., Tafti, M., 2001. The homeostatic regulation of sleep need is under genetic control. J. Neurosci.: Off. J. Soc. Neurosci. 21 (8), 2610–2621.

Franken, P., Tobler, I., Borbély, A.A., 1991. Sleep homeostasis in the rat: simulation of the time course of EEG slow-wave activity. Neurosci. Lett. 130 (2), 141–144.

García-García, F., Yoshida, H., Krueger, J.M., 2004. Interleukin-8 promotes non-rapid eye movement sleep in rabbits and rats. J. Sleep Res. 13 (1), 55–61.

Grønli, J., Meerlo, P., Pedersen, T.T., Pallesen, S., Skrede, S., Marti, A.R., Mrdalj, J., 2017. A rodent model of night-shift work induces short-term and enduring sleep and electroencephalographic disturbances. J. Biol. Rhythm. 32 (1), 48–63.

Gumenyuk, V., Howard, R., Roth, T., Korzyukov, O., Drake, C.L., 2014. Sleep loss, circadian mismatch, and abnormalities in reorienting of attention in night workers with shift work disorder. Sleep 37 (3), 545–556.

Huber, R., Deboer, T., Tobler, I., 2000. Effects of sleep deprivation on sleep and sleep EEG in three mouse strains: empirical data and simulations. Brain Res. 857 (1–2), 8–19.

Kazemi, R., Haidarimoghadam, R., Motamedzadeh, M., Golmohamadi, R., Soltanian, A., Zoghipaydar, M.R., 2016. Effects of shift work on cognitive performance, sleep quality, and sleepiness among petrochemical control room operators. J. Circadian Rhythm. 14, 1.

Kecklund, G., Axelsson, J., 2016. Health consequences of shift work and insufficient sleep. BMJ 355, i5210.

Kemp, B., Kamphuisen, H.A., 1986. Simulation of human hypnograms using a Markov chain model. Sleep 9 (3), 405–414.

Kjellsson, M.C., Ouellet, D., Corrigan, B., Karlsson, M.O., 2011. Modeling sleep data for a new drug in development using markov mixed-effects models. Pharm. Res. 28 (10), 2610–2627.

Knutsson, A., 2003. Health disorders of shift workers. Occup. Med. 53 (2), 103–108.

Kostyalik, D., Vas, S., Kátai, Z., Kitka, T., Gyertyán, I., Bagdy, G., Tóthfalusi, L., 2014. Chronic escitalopram treatment attenuated the accelerated rapid eye movement sleep transitions after selective rapid eye movement sleep deprivation: a model-based analysis using Markov chains. BMC Neurosci. 15 (1). http://dx.doi.org/10.1186/s12868-014-0120-8.

Lo, C.-C., Chou, T., Penzel, T., Scammell, T.E., Strecker, R.E., Stanley, H.E., Ch. Ivanov, P., 2004. Common scale-invariant patterns of sleep-wake transitions across mammalian species. Proc. Natl. Acad. Sci. 101 (50), 17545–17548.

Marti, A.R., Meerlo, P., Grønli, J., van Hasselt, S.J., Mrdalj, J., Pallesen, S., Skrede, S., 2016. Shift in food intake and changes in metabolic regulation and gene expression during simulated night-shift work: a rat model. Nutrients 8 (11). http://dx.doi.org/10.3390/nu8110712.

Morrow, J.D., Opp, M.R., 2005. Sleep-wake behavior and responses of interleukin-6-deficient mice to sleep deprivation. Brain Behav. Immun. 19 (1), 28–39.

Neckelmann, D., Ursin, R., 1993. Sleep stages and EEG power spectrum in relation to acoustical stimulus arousal threshold in the rat. Sleep 16 (5), 467–477.
Opperhuizen, A.-L., van Kerkhof, L.W.M., Proper, K.I., Rodenburg, W., Kalsbeek, A., 2015. Rodent models to study the metabolic effects of shiftwork in humans. Front. Pharmacol. *6*. http://dx.doi.org/10.3389/fphar.2015.00050.
Pilcher, J.J., Lambert, B.J., Huffcutt, A.I., 2000. Differential Effects of Permanent and Rotating Shifts on Self-Report Sleep Length: a Meta-Analytic Review. Sleep *23* (2), 1–9.
Postnova, S., Layden, A., Robinson, P.A., Phillips, A.J.K., Abeysuriya, R.G., 2012. Exploring sleepiness and entrainment on permanent shift schedules in a physiologically based model. J. Biol. Rhythm. *27* (1), 91–102.
Pratesi, A., 2013. Skeletal muscle: an endocrine organ. Clinical cases in mineral and bone metabolism. Off. J. Ital. Soc. Osteoporos. Miner. Metab. Skelet. Dis. http://dx.doi.org/10.11138/ccmbm/2013.10.1.011.
Rempe, M.J., Wisor, J.P., 2014. Cerebral lactate dynamics across sleep/wake cycles. Front. Comput. Neurosci. 8, 174.
Salgado-Delgado, R., Ángeles-Castellanos, M., Buijs, M.R., Escobar, C., 2008. Internal desynchronization in a model of night-work by forced activity in rats. Neuroscience 154 (3), 922–931.
St Hilaire, M.A., Klerman, E.B., Khalsa, S.B.S., Wright Jr, K.P., Czeisler, C.A., Kronauer, R.E., 2007. Addition of a non-photic component to a light-based mathematical model of the human circadian pacemaker. J. Theor. Biol. 247 (4), 583–599.
Torsvall, L., Akerstedt, T., 1987. Sleepiness on the job: continuously measured EEG changes in train drivers. Electroencephalogr. Clin. Neurophysiol. 66 (6), 502–511.
Torsvall, L., Akerstedt, T., Gillander, K., Knutsson, A., 1989. Sleep on the night shift: 24-hour EEG monitoring of spontaneous sleep/wake behavior. Psychophysiology 26 (3), 352–358.
Trachsel, L., Tobler, I., Achermann, P., Borbély, A.A., 1991. Sleep continuity and the REM-nonREM cycle in the rat under baseline conditions and after sleep deprivation. Physiol. Behav. 49 (3), 575–580.
Ursin, R., Baste, V., Moen, B.E., 2009. Sleep duration and sleep-related problems in different occupations in the Hordaland Health Study. Scand. J. Work Environ. Health 35 (3), 193–202.
van Diepen, H.C., Lucassen, E.A., Yasenkov, R., Groenen, I., Ijzerman, A.P., Meijer, J.H., Deboer, T., 2014. Caffeine increases light responsiveness of the mouse circadian pacemaker. Eur. J. Neurosci. 40 (10), 3504–3511.
Van Dongen, H.P.A., Balkin, T.J., Hursh, S.R., 2017. Performance deficits during sleep loss and their operational consequences. Princ. Pract. Sleep. Med. 682–688.e4.
Vyazovskiy, V.V., Achermann, P., Tobler, I., 2007. Sleep homeostasis in the rat in the light and dark period. Brain Res. Bull. 74 (1–3), 37–44.
Vyazovskiy, V.V., Tobler, I., 2012. The temporal structure of behaviour and sleep homeostasis. PLoS One 7 (12), e50677.
Yang, M.C., Hursch, C.J., 1973. The use of a semi-Markov model for describing sleep patterns. Biometrics 29 (4), 667–676.
Yassouridis, A., Steiger, A., Klinger, A., Fahrmeir, L., 1999. Modelling and exploring human sleep with event history analysis. J. Sleep. Res. 8 (1), 25–36.
Zung, W.W., Naylor, T.H., Gianturco, D.T., Wilson, W.P., 1965. Computer simulation of sleep EEG patterns with a Markov chain model. Recent Adv. Biol. Psychiatry 8, 335–355.